Scientific Report

TRANSPARENT PROCESS

EMBO reports

# Loss of the canonical spindle orientation function in the Pins/LGN homolog AGS3

Mehdi Saadaoui[1,*,†], Daijiro Konno[2], Karine Loulier[3], Rosette Goiame[1], Vaibhav Jadhav[4], Marina Mapelli[4], Fumio Matsuzaki[2] & Xavier Morin[1,**]

## Abstract

**In many cell types, mitotic spindle orientation relies on the canonical "LGN complex" composed of Pins/LGN, Mud/NuMA, and G$\alpha_i$ subunits. Membrane localization of this complex recruits motor force generators that pull on astral microtubules to orient the spindle. *Drosophila* Pins shares highly conserved functional domains with its two vertebrate homologs LGN and AGS3. Whereas the role of Pins and LGN in oriented divisions is extensively documented, involvement of AGS3 remains controversial. Here, we show that AGS3 is not required for planar divisions of neural progenitors in the mouse neocortex. AGS3 is not recruited to the cell cortex and does not rescue LGN loss of function. Despite conserved interactions with NuMA and G$\alpha_i$ *in vitro*, comparison of LGN and AGS3 functional domains *in vivo* reveals unexpected differences in the ability of these interactions to mediate spindle orientation functions. Finally, we find that *Drosophila* Pins is unable to substitute for LGN loss of function in vertebrates, highlighting that species-specific modulations of the interactions between components of the Pins/LGN complex are crucial *in vivo* for spindle orientation.**

**Keywords** AGS3; LGN; Pins; spindle orientation; vertebrate neuroepithelium
**Subject Categories** Cell Adhesion, Polarity & Cytoskeleton; Cell Cycle; Evolution
**DOI** 10.15252/embr.201643048 | Received 12 July 2016 | Revised 14 May 2017 | Accepted 19 May 2017 | Published online 6 July 2017
**EMBO Reports (2017) 18: 1509–1520**

## Introduction

Oriented cell divisions (OCD) play an essential role in the development, growth, and homeostasis of many tissues [1,2]. They rely on the specific orientation of the mitotic spindle during mitosis, which controls the position of the cleavage plane and hence the position of the two daughter cells within the tissue. In many cell types, OCD relies on an evolutionary conserved protein complex composed of Pins/LGN, Mud/NuMA, and G$\alpha_i$ subunits of heterotrimeric G proteins. In response to intra- or extracellular polarity cues, a local enrichment of this complex at specific cortical regions of the dividing cell is used to recruit motor proteins of the dynein/dynactin complex [3–5]. This creates an imbalance in cortical forces exerted on astral microtubules and drives mitotic spindle movements and orientation [1,6].

A conserved role for Pins and its homolog LGN [7] in mitotic spindle orientation has been largely documented in *Drosophila* and vertebrates [8–12]. In particular, mouse LGN was able to substitute for Pins and rescue both spindle orientation and associated asymmetric cell division defects of embryonic neuroblasts in a *Drosophila pins* mutant background [13]; in addition to this role in spindle orientation, mouse LGN has been involved in the regulation of G protein-activated inwardly rectifying potassium (GIRK) channels [14], and in regulating spine density in cortical neurons [15], a function that requires its ability to interact with MAGUK proteins of the Dlg family. LGN is also essential for the establishment of the planar polarization and the organization of stereocilia bundles in cochlear hair cells [16–18], and LGN mutations have been associated with deafness in mice and humans [19–21].

In addition to LGN, the canonical *Drosophila* Pins possesses another homologous gene in vertebrates named AGS3 [22]. AGS3 has been studied in a number of cell types *in vitro* and in a mouse loss-of-function model, and implicated in a diverse set of cellular, organ, and physiological functions, ranging from autophagy, Golgi apparatus organization, protein trafficking, and drug craving, but a clear picture of its cellular function has yet to emerge [23]. In addition, LGN and/or AGS3 show polarized recruitment and may be functionally involved in heterotrimeric G-protein-dependent chemotaxis of mouse neutrophils [24].

All three genes belong to the type II class of receptor-independent activator of G-protein signaling (AGS) family [23]. They share extensive sequence, structure homology, and biochemical interactions

1 Cell Division and Neurogenesis Group, Ecole Normale Supérieure, CNRS, Inserm, Institut de Biologie de l'Ecole Normale Supérieure (IBENS), PSL Research University, Paris, France
2 Laboratory for Cell Asymmetry, RIKEN Center for Developmental Biology, Chuo-ku, Kobe, Japan
3 UPMC Université Paris 06, Sorbonne Universités, CNRS, Inserm, Institut de la Vision, Paris, France
4 Department of Experimental Oncology, European Institute of Oncology, Milan, Italy
*Corresponding author. Tel: +33 1 45 68 81 54; E-mail: mehdi.saadaoui@pasteur.fr
**Corresponding author. Tel: +33 1 44 32 37 29; E-mail: xavier.morin@ens.fr
†Present address: Morphogenesis in Higher Vertebrates, Developmental and Stem Cell Biology, Institut Pasteur, Paris, France

© 2017 The Authors

(Fig 1A) [13]. Their N-terminal TPR domain (containing eight tetratricopeptide repeats, seven of which contain a leucine–glycine–asparagine motif which gave LGN its name) is involved in multiple protein–protein interactions, and in particular in the interaction with NuMA, which is crucial for the spindle orientation function. The C-terminal GPR (G-protein regulatory) region contains three (in Pins) or four (in LGN and AGS3) GoLoco motifs; GoLoco are 15- to 20-aa $G\alpha_i$/o-interacting domains with a guanine dissociation inhibitory activity [25,26]. Within the GPR region, GoLoco motifs are separated by 11- to 25-aa-long sequences that are thus far thought to mainly serve as spacers allowing the simultaneous interaction of the GPR region with multiple $G\alpha_i$ subunits [23]. A less conserved linker region separates the TPR and GPR domains. Recently, we have shown that the direct interaction between the phosphorylated linker domain of LGN and the baso-lateral protein Dlg1/SAP97 is crucial for mitotic spindle orientation in chick neuroepithelial progenitors and cultured HeLa cells [27], a function that is conserved in its ortholog Dlg in some fly epithelial tissues [28].

AGS3 and LGN probably appeared through the duplication of a common Pins-like ancestor and they have clearly evolved new and different functions, through the acquisition of specific interactions [23]. This raises the question of whether only one of them, or both, retained the capacity to control spindle orientation. Interestingly, while the linker region of AGS3 does not interact with Dlg family members [15,29], one previous study proposed a role for AGS3 during mitotic spindle orientation in the mouse embryonic cortex [30], but the mechanism is unclear.

In this study, we explored whether LGN and AGS3 have both retained the "spindle orientation" function of their common ancestor. We first observed that AGS3 is not required for planar spindle orientation in a mouse knockout line, and that AGS3 is not recruited to the cell cortex in mouse neural progenitors. We then used the LGN-dependent planar divisions of neural progenitors in the chick neural tube as an *in vivo* model to compare the functions of LGN and AGS3, and found that AGS3 cannot substitute for LGN. In-depth analysis through multiple AGS3/LGN chimeras showed that differences in several functional domains contribute to AGS3's loss of the ability to control mitotic spindle orientation. Remarkably, we also found that *Drosophila* Pins was unable to substitute for LGN in vertebrates, despite the interchangeability of both molecules in the fly. Our study suggests that despite similar binding affinities observed between LGN and AGS3 and their common interaction partners *in vitro*, other as yet unidentified partners are required to allow these interactions to occur *in vivo*.

## Results and Discussion

### AGS3 is cytoplasmic during progenitor division and is not able to rescue LGN loss of function

Since LGN and AGS3 share extensive domain composition and sequence homology (Fig 1A), it has been proposed that both molecules may share functional properties and that both could be involved in spindle orientation. We generated a mouse AGS3 mutant strain lacking the GPR region (AGS3ΔC, Fig EV1) and investigated spindle orientation in mouse cortical progenitors. Remarkably, the orientation of divisions in anaphase was undistinguishable between control and AGS3ΔC mutant cells (Fig 1B), in agreement with our previous observations using siRNA (unpublished and [8]) but in contrast to a previous report [30]. To better characterize this functional difference, we compared the localization of GFP-LGN and GFP-AGS3 fusion proteins during mitosis in several cell types known to rely on LGN for their spindle orientation [8,9,11]. In radial glial cells of the mouse embryonic cortex, in chick embryonic spinal cord neural progenitors, and in MDCK cells, AGS3 failed to be recruited to the cell cortex during mitosis (Fig 1C–E). By contrast, LGN was consistently enriched at the cortex in all three cell types, consistent with its well-documented role in recruiting cortical force generators and its requirement for planar cell division in both mouse and chick neural progenitors. The knockout phenotype and the different localization of the two molecules suggest that AGS3 and LGN do not play a redundant role in spindle orientation in these cells.

We previously reported that full-length AGS3 is not produced in the chick, due to a frame shift in the coding sequence [9]. We thought of using this characteristic to our advantage by exploring LGN and AGS3 functional divergences in the chick neural tube. Throughout this study, we used mouse AGS3 and mouse LGN cDNAs in functional and localization experiments *in vivo*. Subcellular distribution was performed in dividing chick neuroepithelial progenitors by *in ovo* electroporation using low-level expression of GFP-tagged molecules from the weak CMV promoter, in order to avoid saturation of the cell and potential localization artifacts. By contrast, rescue and gain-of-function experiments were performed with "high-level" expression from the strong CAG promoter. In particular, we have previously shown that mouse LGN is able to rescue the LGN RNAi phenotype in the chick neural tube [9] (see also Fig 1F and G). Besides, whereas *in vitro* studies have described that overexpression of LGN induced defects in spindle orientation relative to the adhesion substrate in HeLa cells [4] and exaggerated spindle rocking in MDCK cells [31], we reported that overexpression of mouse LGN *in vivo* from the CAG promoter does not prevent planar spindle orientation in the neural tube [9] (see also Fig 1H).

In agreement with its cytoplasmic distribution in mitotic neuroepithelial cells, AGS3 was unable to substitute for LGN and failed to rescue spindle orientation defects resulting from LGN knockdown, whereas expression of LGN restored planar spindle orientation (Fig 1F and G for quantification). In addition, we controlled whether AGS3 misexpression may exert a dominant negative effect: like LGN, AGS3 expression in a wild-type (wt) background did not cause any spindle orientation defect (Fig 1H).

AGS3 and LGN may compete for the interaction with $G\alpha_i$ subunits at the cell cortex: We therefore analyzed the distribution of GFP-AGS3 in an LGN RNAi background. However, even in the absence of LGN, AGS3 remained cytoplasmic in chick neuroepithelial cells (Fig EV3A). As the two proteins share strong sequence homology, domain composition, and extensive structural similarities, we decided to explore the molecular basis for this functional difference.

### The linker domain of LGN does not confer the ability to regulate mitotic spindle orientation to AGS3

We have previously established that a direct interaction between LGN and the baso-lateral protein Dlg1 is necessary for the mitotic

 © 2017 The Authors

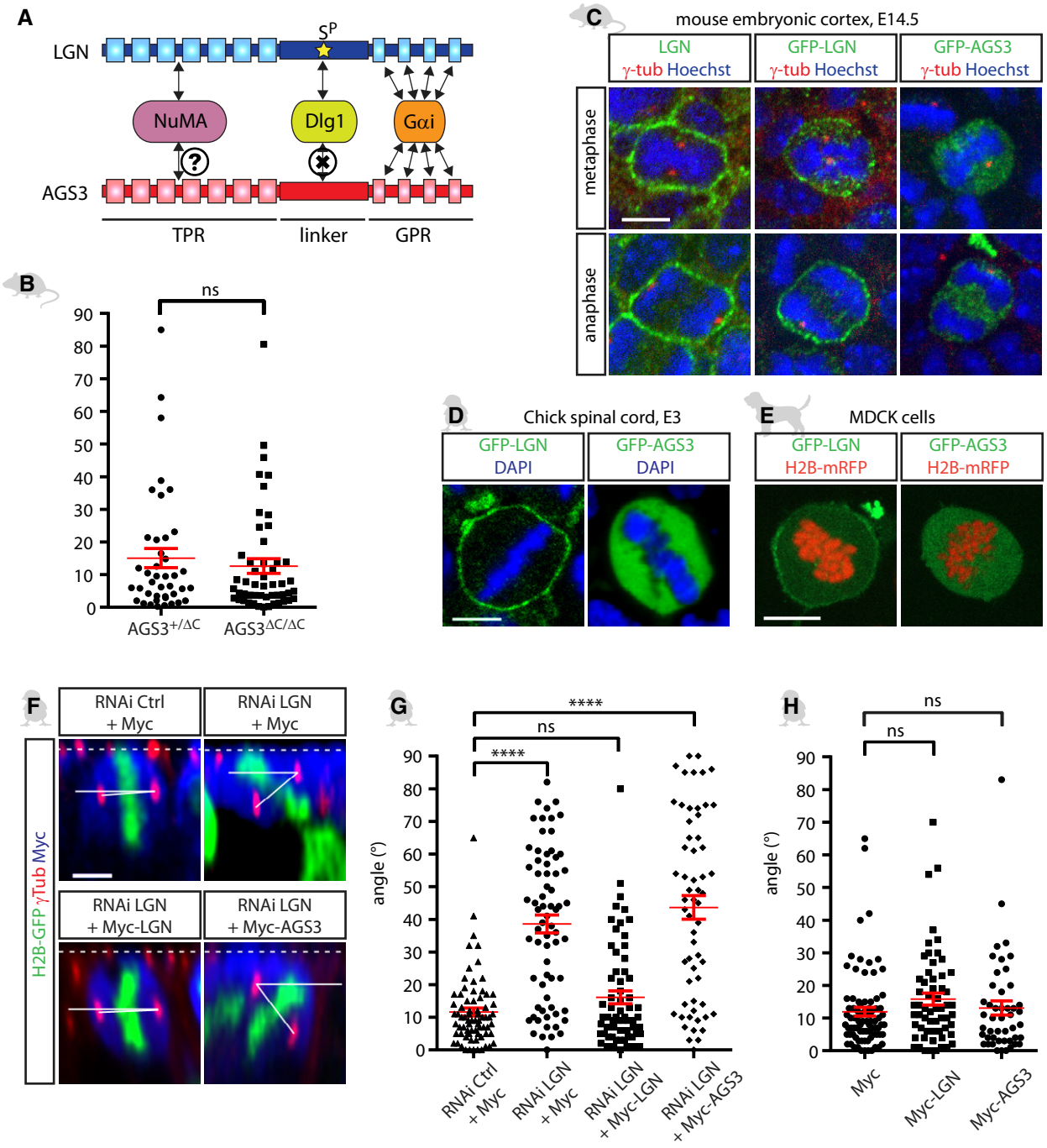


**Figure 1. The LGN homolog AGS3 is cytoplasmic and does not regulate mitotic spindle orientation in the vertebrate neuroepithelium.**

A LGN/AGS3 protein structure and functional domains required for interaction with NuMA, Dlg1, and $G\alpha_i$. The black cross and question mark, respectively, point toward absent or uncharacterized interaction.

B Spindle orientation in anaphase is normal in radial glial cells of AGS3ΔC mice at E14.5 (mean ± SEM, $n$ = 41 and 51 cells from 3 and 4 embryos, respectively; ns = not significant, Mann–Whitney test).

C In mouse radial glial cells at E14.5, both endogenous LGN and a GFP-mLGN fusion protein accumulate at the cell cortex whereas GFP-mAGS3 is cytoplasmic throughout mitosis.

D, E GFP-mLGN is cortical and GFP-mAGS3 is cytoplasmic in dividing chick neural progenitors at E3 (D) and in MDCK cells (E).

F Z-view examples of typical spindle orientation observed upon LGN RNAi and rescue experiments with different LGN and AGS3 constructs in chick neural progenitors at E3. The dashed lines indicate the apical surface and the solid lines the mitotic spindle angle.

G, H Quantification of mitotic spindle angles in LGN RNAi rescue experiment (G) or after misexpression in a wt background (H) in the chick spinal cord (mean ± SEM, $n$ > 50 cells from at least three different embryos per condition; ns = not significant, ****$P$ < 0.0001, Mann–Whitney test).

Data information: Scale bars: 5 μm in all panels except panel (E) (10 μm).

© 2017 The Authors

spindle orientation function of LGN in the chick neural tube [27]. This interaction relies on the 130-amino-acid-long linker domain of LGN, and *in vitro* experiments have defined a short peptide of 18 aa containing a core RRHpS motif inside the linker as a binding interface between LGN and the C-terminal guanylate kinase (GK) domain of Dlg (Fig 2A) [29]. Neither the AGS3 linker nor a short AGS3 peptide encompassing the same region is able to interact with Dlg [15,29]. Phosphorylation of the serine in the RRHpS motif is essential for interaction with Dlg GK domain *in vitro* [29], and a serine to alanine substitution in this motif strongly reduces the cortical recruitment of full-length LGN and abolishes its spindle orientation capability *in vivo* [27]. The crucial serine residue is conserved between LGN and AGS3. However, the arginine (R) residue localized at position −3, an essential element of the consensus R-X-X-S/T sequence recognized by multiple kinases, is replaced by a glutamine (Q) in AGS3; besides, an alanine substitution at this position in the PhosphoLGN peptide caused a fivefold decrease in the binding affinity between LGN and Dlg, even though the peptide contained a phosphorylated serine in these experiments [29]. We therefore reasoned that the ability of AGS3 to be phosphorylated on this particular serine residue is impaired, but that a Q-R substitution in AGS3 may restore phosphorylation of the linker domain, promote interaction with Dlg1, and confer LGN-like spindle orientation properties to AGS3. However, a GFP fusion to $AGS3^{QR}$ still displayed a cytoplasmic localization in neuroepithelial cells (Fig 2B), and $AGS3^{QR}$ was unable to rescue spindle orientation defects in an LGN knockdown background (Fig 2C and D). We then swapped increasing parts of the linker domain between LGN and AGS3 (Figs 2 and EV2). To our surprise, even a complete replacement of the linker did not change the cytoplasmic localization of the GFP-tagged $AGS3^{LGN\text{-}linker}$ chimera (Fig 2B). Likewise, $AGS3^{LGN\text{-}linker}$ expression did not rescue spindle orientation in an LGN RNAi background (Fig 2C and D). Hence, the inability of AGS3 to interact with Dlg1 is not sufficient to explain its inability to control spindle orientation.

In line with this conclusion, we also found that overexpression of $AGS3^{QR}$ and $AGS3^{LGN\text{-}linker}$, respectively, caused mild—but significant—and strong spindle misorientation (Fig EV3B). This dominant effect may be explained by a competition between these constructs and endogenous LGN for the interaction with Dlg1 combined to their inability to interact with one or more other LGN partners. Consistent with this hypothesis, expression of $AGS3^{LGN\text{-}linker}$ led to the cytoplasmic accumulation of a GFP-Dlg1 construct compared to the control situation, although GFP-Dlg1 was still observed at the cell cortex (Fig EV3C). We therefore set out to identify other important differences between LGN and AGS3.

### Differential cortical recruitment of the GPR domains of LGN and AGS3 in mitotic progenitors *in vivo*

We have previously shown that both linker and GPR domains of LGN are required for its cortical recruitment. In particular, a mutated LGN that is unable to interact with Dlg1 ($LGN^{SA}$) still displays residual cortical recruitment [27,32]. By contrast, we did not detect any cortical staining with AGS3 (Figs 1B and 2B). This suggested that the GPR domain of AGS3 may not be able to mediate cortical recruitment and led us to ask whether the GPR domains of LGN and AGS3 are functionally distinct. We generated a chimeric construct in which the GPR domains of LGN were replaced by those of AGS3 ($LGN^{AGS3\text{-}GPR}$). A GFP-tagged version of this chimera displayed a cytoplasmic localization, both in mouse radial glial cells (Fig 3A) and in chick neuroepithelial progenitors (Fig 3B). Remarkably, co-expression of $G\alpha_i$ led to a strong cortical recruitment of $LGN^{AGS3\text{-}GPR}$ in mouse radial glial cells (Fig 3A). This suggested that AGS3 GPR domain does not interact with cortical $G\alpha_i$ subunits *in vivo*. Accordingly, the chimera was unable to rescue the LGN loss-of-function phenotype in the chick neuroepithelium (Fig 3C). In addition, when overexpressed in a wild-type background, $LGN^{AGS3\text{-}GPR}$ caused a dominant spindle misorientation phenotype (Fig 3D) similar to the dominant effect of the $AGS3^{LGN\text{-}linker}$ construct described above (Fig EV3B). Remarkably, when Myc-tagged $LGN^{AGS3\text{-}GPR}$ was expressed in combination with GFP-$LGN^{wt}$, the latter was poorly recruited to the cell cortex (Fig 3E); this suggests that the dominant phenotype results from a competition with endogenous LGN for interaction with other partners, most likely Dlg1 but also possibly NuMA, reducing LGN cortical recruitment and preventing the formation of a functional $G\alpha_i$/LGN/NuMA complex at the cortex. Indeed, GFP-Dlg1 was also enriched in the cytoplasm in these cells (Figs 3E and EV3C). The inability of the chimera to localize to the cortex could be due to its failure to switch from an inactive, closed state (where TPR and GPR domains interact together intramolecularly and bind poorly to $G\alpha_i$ and NuMA) to an open active conformation [31,33], or to a reduced affinity of the GPR toward $G\alpha_i$. We addressed the second point by comparing the distribution of GFP-tagged GPR domains alone from LGN and AGS3 during progenitor division. Whereas $GPR^{LGN}$ was enriched at the cell cortex as reported previously [27], $GPR^{AGS3}$ was cytoplasmic (Fig 3F, upper panels).

Experiments *in vitro* have reported that individual GoLoco motifs from AGS3 and LGN present similar binding affinity toward $G\alpha_i$ subunits. While the core 19 amino acid GoLoco motif only shows weak affinity, experiments with "extended" GoLoco sequences including six to 35 additional amino acids C-terminal to the core GoLoco motif have shown that these downstream sequences modulate the binding of individual GoLoco motifs [34,35], indicating that they may contribute to the global affinity of the protein toward $G\alpha_i$. However, the *in vitro* affinity of the whole purified GPR domains toward $G\alpha_i$ appeared very similar between LGN and AGS3, although marginally higher for LGN [36].

We therefore wondered whether a conformational difference related to the sequences separating individual GoLoco motifs (thereafter called interdomains) in LGN and AGS3 might be responsible for differential accessibility to cortical $G\alpha_i$ subunits *in vivo*. To test this idea, we generated complete chimeras within the GPR domains of AGS3 and LGN, in which we swapped the four GoLoco domains between AGS3 and LGN, leaving interdomains unchanged, and vice versa. Indeed, we found that the chimera containing the GoLoco domains of AGS3 and the interdomains of LGN ($GPR^{AGS3interLGN}$) was recruited to the cortex as efficiently as $GPR^{LGN}$, while the converse construct ($GPR^{LGNinterAGS3}$) was essentially cytoplasmic, similar to $GPR^{AGS3}$ (Fig 3F and G). Similarly, a Myc-tagged version of full-length LGN in which only the GoLoco had been replaced by those from AGS3 ($LGN^{AGS3Goloco}$) was recruited to the cortex, whereas a construct containing only the interdomains from AGS3 ($LGN^{AGS3interdomain}$) remained cytoplasmic (Fig 3H). Surprisingly, when expressed in an LGN RNAi background, $LGN^{AGS3Goloco}$ did not rescue the spindle orientation

 © 2017 The Authors

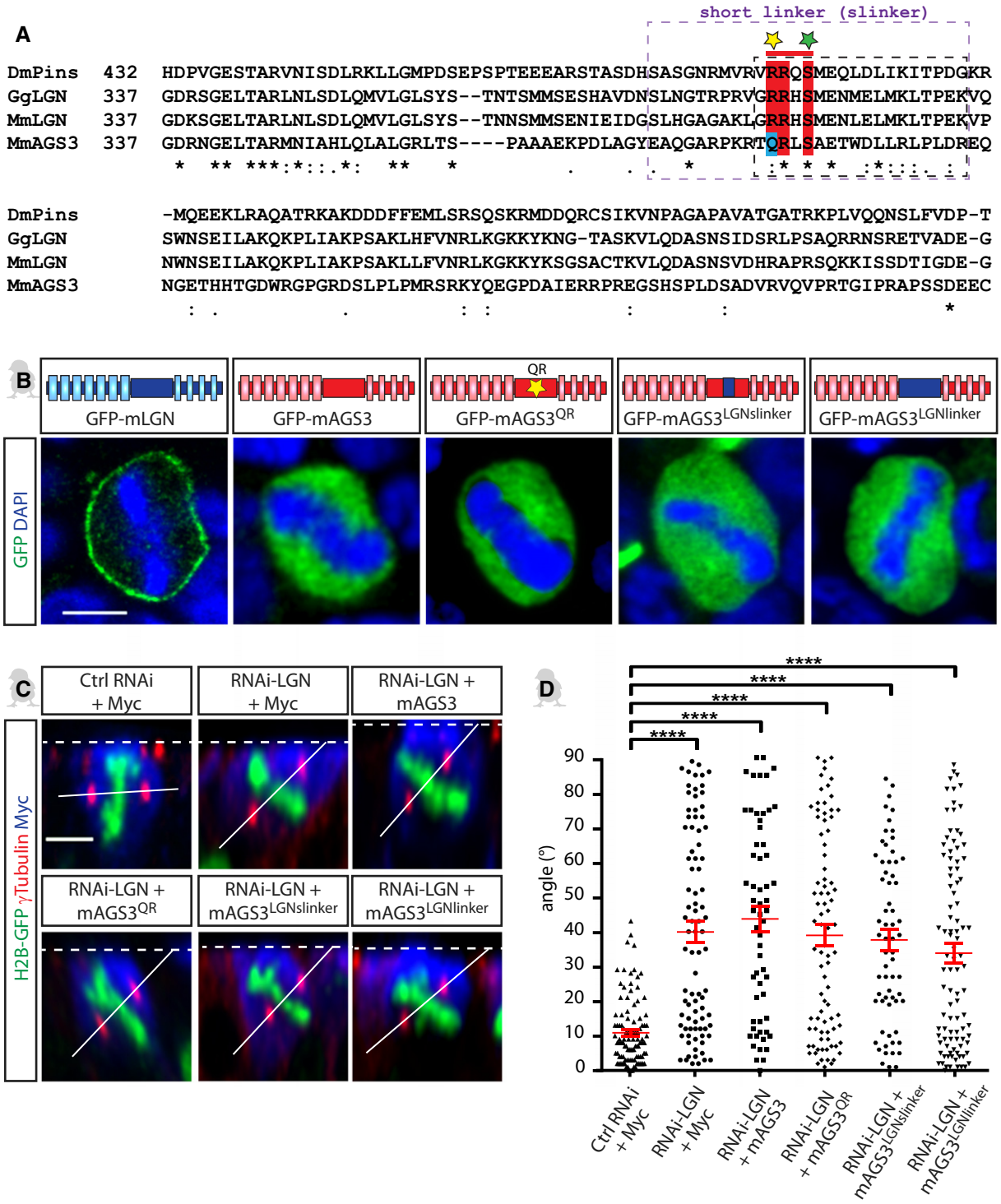


**Figure 2. The linker domain of LGN does not confer mitotic spindle activity to AGS3.**

A Linker domain sequence alignment of four representative Pins homologs. Green star: phosphorylated serine residue (in Pins and LGN); yellow star: conserved arginine residue in the RRxpS consensus kinase recognition motif. In AGS3, this arginine is replaced with a glutamine residue; black dotted box: peptide sequence used for binding studies in [29]; pink dotted box: short linker sequence used in the mAGS3$^{LGNsLinker}$ chimeric construct. Species abbreviations are: Dm Drosophila *melanogaster*, Gg *Gallus gallus*, Mm *Mus musculus*.

B Replacing increasing portions of AGS3 linker domain with LGN-specific residues is not sufficient to induce cortical localization of GFP-AGS3 fusion constructs in dividing neural progenitors. A scheme above each construct name depicts the structure of the chimeras.

C Z-view examples of typical spindle orientation observed for each condition. The dashed lines indicate the apical surface and the solid lines the mitotic spindle angle.

D Quantification of the mitotic spindle angles (mean ± SEM, $n > 60$ cells; ****$P < 0.0001$, Mann–Whitney test).

Data information: Scale bars: 5 μm in all panels.

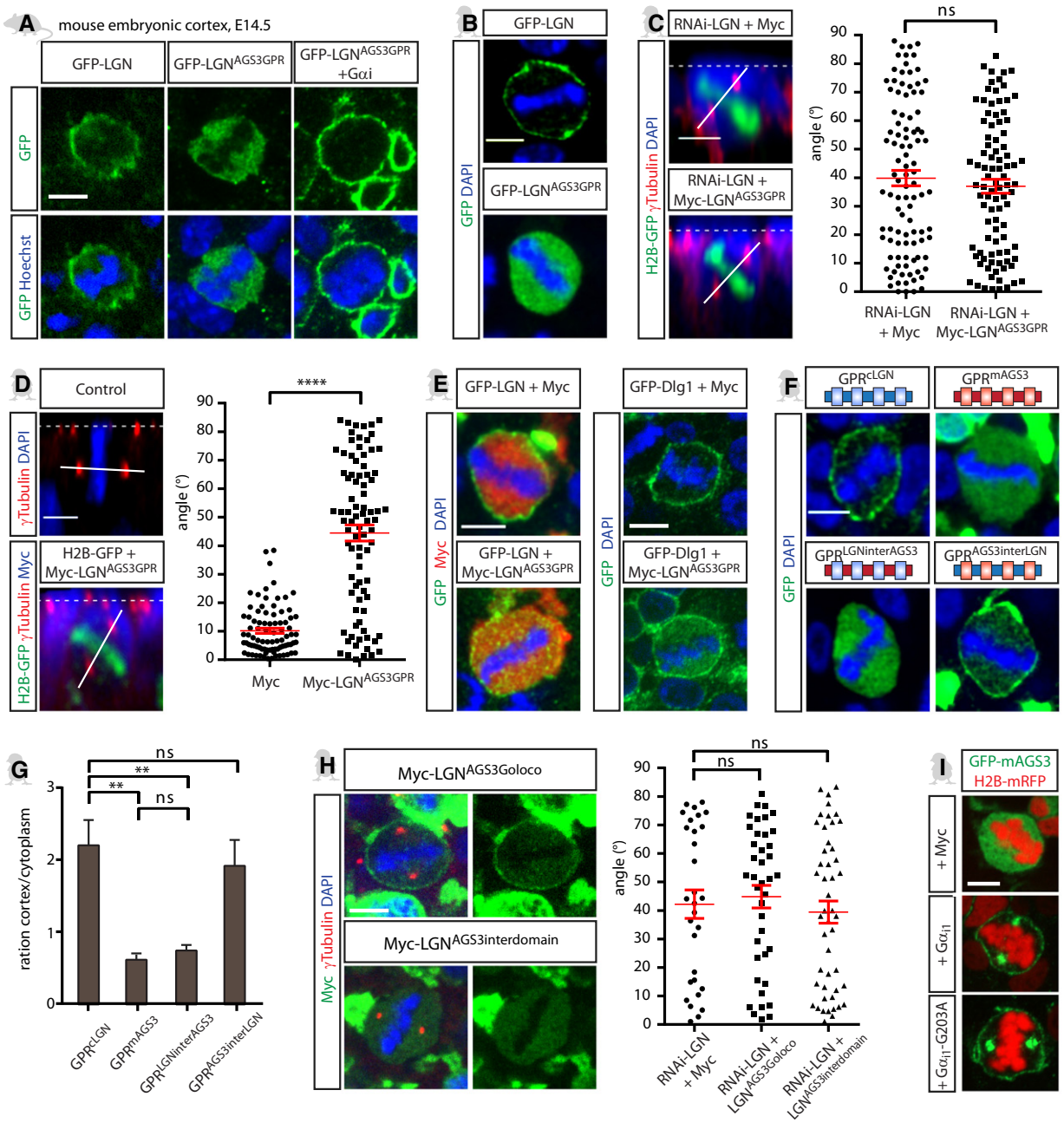


**Figure 3. GPR domains of LGN and AGS3 are functionally distinct *in vivo*.**

A, B Replacing the GPR domains of LGN with those of AGS3 ($LGN^{AGS3\text{-}GPR}$ chimera) delocalizes LGN from cell cortex to cytoplasm in both mouse (A) and chick (B) neural progenitors. However, overexpressed $G\alpha_i1$ recruits $LGN^{AGS3\text{-}GPR}$ to the cell membrane (A).

C $LGN^{AGS3\text{-}GPR}$ is unable to rescue spindle orientation defects in an LGN RNAi background (mean ± SEM, $n > 60$ cells; ns = not significant, Mann–Whitney test).

D Ectopic expression of $LGN^{AGS3\text{-}GPR}$ randomizes spindle orientation in a wt background (mean ± SEM, $n = 85$ cells; ****$P < 0.0001$, Mann–Whitney test).

E GFP-LGN is partially delocalized from cell cortex to cytoplasm, and GFP-Dlg1 is stronger in the cytoplasm upon expression of $LGN^{AGS3\text{-}GPR}$.

F, G Localization of GPR domain fusion constructs reveals that binding ability of GoLoco domains to cortical $G\alpha_i$-GDP requires specific interdomain sequences. AGS3 interdomains induce cytoplasmic localization while LGN interdomains lead to cortical enrichment of LGN/AGS3 GPR domains. The ratio between cortical and cytoplasmic distribution of the different constructs is provided in (G) (see Materials and Methods for detail of quantification; mean ± SEM, $n > 8$ cells/condition; ns = not significant, **$P < 0.01$, one-way ANOVA test with multiple comparisons).

H A full-length LGN with AGS3 GoLoco domains ($Myc\text{-}LGN^{AGS3\text{-}GoLoco}$) is cortical, (top), whereas full-length LGN with AGS3 interdomains ($Myc\text{-}LGN^{AGS3\text{-}interdomain}$) is cytoplasmic (bottom). None of these constructs rescues the LGN RNAi spindle orientation phenotype (mean ± SEM, $n > 40$ cells; ns = not significant, Mann–Whitney test).

I Overexpressed wt or GDP-bound G203A mutant forms or $G\alpha_i1$ recruits wt AGS3 to the cell membrane.

Data information: Scale bars: 5 μm in all panels. The dashed lines indicate the apical surface and the solid lines the mitotic spindle angle (C, D).

 © 2017 The Authors

phenotype, indicating that the observed cortical recruitment is not sufficient to restore spindle orientation ability to the full-length chimera. One possible explanation is that in addition to cortical recruitment, the GoLoco motifs may have additional functions in the context of the full-length molecule: in particular, they may be involved in the strength of the intramolecular GPR–TPR interaction [31,33], therefore modulating the ability to switch from closed to open conformation and the formation of a complex with NuMA and $G\alpha_i$ subunits. It should be noted that GoLoco domains in our chimeras are 23-amino-acid-long sequences that include one and three amino acids, respectively, at the N-terminal and C-terminal ends of each 19 amino-acids core GoLoco motif. Our data therefore do not discriminate whether differences between core GoLocos of AGS3 and LGN or between the immediate surrounding residues are involved.

Overall, our data show that although individual GoLoco domains interact with $G\alpha_i$ subunits *in vitro*, they are not sufficient on their own for cortical recruitment during mitosis *in vivo*, and that the specific sequence of interdomains in the GPR plays a crucial role. In support of this observation, we found that a single consensus GoLoco motif [26,34] fused to a GFP reporter (GFP-GoLoco) was not recruited to the cortex *in vivo* (Fig EV4A). However, co-expression of $G\alpha_i$-G203A (a point mutant of $G\alpha_i$ that is unable to release GDP, and therefore shows a strong affinity for GoLoco motifs) was sufficient to recruit GFP-GoLoco as well as GFP-$GPR^{AGS3}$ to the cortex (Fig EV4A and B). Similarly, we found that full-length GFP-mAGS3 was strongly recruited to the cell cortex upon overexpression of wt $G\alpha_i$ or $G\alpha_i$-G203A (Fig 3I). This indicates that in mitotic progenitors *in vivo*, endogenous $G\alpha_i$-GDP levels combined with the intrinsic affinity of AGS3 or LGN GoLoco domains alone for $G\alpha_i$ subunits are not sufficient for cortical recruitment. The interdomains contribute to the conformation of LGN and regulate its cortical recruitment *in vivo*, either by favoring the accessibility of GoLoco domains for $G\alpha_i$-GDP binding, or through the interaction of the interdomains with an as yet unknown partner that facilitates LGN transport to the cortex.

### The TPR domains of AGS3 can only partially substitute functionally those of LGN

Having shown that both linker and GPR domains of AGS3 and LGN carry essential differences regarding spindle orientation, we sought to investigate whether the highly conserved N-terminal TPR domains also contribute to their functional specificity. Although the conservation of TPR interaction with NuMA has been postulated, it has not been formally shown. Using recombinant proteins, we found that TPR domains of AGS3 indeed interact with NuMA *in vitro* (Fig EV5). We then replaced the TPR domain of LGN with that of AGS3, and investigated the subcellular distribution of a GFP-tagged version of the chimera ($LGN^{AGS3\text{-}TPR}$). Remarkably, unlike all other chimeric constructs tested in this study, $LGN^{AGS3\text{-}TPR}$ displayed a cortical distribution in mitotic cells similar to the localization of wt LGN, confirming that both linker and GPR domains of LGN are necessary for its correct cortical localization (Fig 4A). However, unlike wt LGN, $LGN^{AGS3\text{-}TPR}$ rescued only partially the spindle orientation phenotypes in an LGN RNAi background ($\alpha_{Zmean} = 28.7°$ compared to 39.8° observed in LGN loss of function, Fig 4B). Besides, overexpression of $LGN^{AGS3\text{-}TPR}$ in a wild-type background caused a mild dominant effect ($\alpha_{Zmean} = 21.5°$) and delocalized a GFP-LGN fusion construct from cell cortex to cytoplasm (Fig 4C and D). This suggests that despite its correct cortical localization, the $LGN^{AGS3\text{-}TPR}$ chimera differs in the ability of its TPR domains to interact with specific partners. This prevents the generation of the adequate level of force to properly orient the spindle, and the chimera competes with endogenous LGN in this task.

To gain insight into TPR functional differences, we compared the localization of TPR from LGN and AGS3 in chick neuroepithelial cells. While GFP-$TPR^{AGS3}$ accumulated at the spindle poles, presumably via NuMA interaction, GFP-$TPR^{LGN}$ presented a cytoplasmic distribution. This suggests a difference between the two TPR domains in their ability to interact with the pool of NuMA that locates at the spindle *in vivo* (Fig 4E). In addition to the interaction with NuMA and the intramolecular interaction with the GPR domains, the TPR domains of LGN and AGS3 have been shown to interact with Inscuteable [37–39] and Frmpd1 [38,40]. It was also shown recently that Afadin-6 binds LGN-TPR domains in a manner competitive to NuMA [41]. Hence, the TPR domain emerges as an interaction platform whose specific organization may recruit additional partners that remain to be identified. Both Afadin-6 and Insc interactions are involved in the cortical localization of LGN. Despite the high sequence conservation between AGS3 and LGN, discrete changes in the amino acid sequence of the TPR region may modulate their relative affinity for these partners, which may account for the different localization of the TPR domains in dividing cells, and ultimately in the reduced ability of the $LGN^{AGS3\text{-}TPR}$ chimera to control planar spindle orientation.

### *Drosophila* Pins expression in the neuroepithelium cannot substitute for LGN and has a dominant negative effect

Our data so far show important functional differences in all three main domains (TPR, linker, and GPR) of AGS3 and LGN regarding the spindle orientation function. AGS3 and LGN probably derive from the duplication of a common ancestor. In *Drosophila*, a unique *pins* gene shares the spindle orientation function with LGN. Mouse LGN can substitute for Pins in asymmetric division of embryonic neuroblasts in a *Drosophila pins* mutant background: LGN recapitulated the apical distribution of Pins, and rescued the spindle orientation defects [13], indicating that LGN can interact in *Drosophila* with the essential Pins partners Mud (NuMA), Inscuteable, and $G\alpha_i$. To complete our analysis, we investigated the localization and activity of fly Pins in the chick neuroepithelium. Surprisingly, YFP-tagged Pins only localized weakly at the cell cortex compared to LGN (Fig 5A). Moreover, Pins did not reciprocate the ability of LGN to rescue *pins* phenotypes, as it was unable to rescue the LGN knockdown phenotype (Fig 5B). Besides, overexpression of Pins had a strong dominant effect resulting in random spindle orientation in the chick neuroepithelium (Fig 5C).

While LGN and AGS3 GPR domains consist of four GoLoco domains, Pins only has three GoLoco domains [13]. The dominant effect might therefore result from the weaker cortical attachment of fly Pins in chick neuroepithelial cells: in this scenario, Pins would be inefficient at generating forces in the neuroepithelium, but may nonetheless compete with endogenous LGN for complex formation. To test this hypothesis, we generated a version of LGN with only

© 2017 The Authors

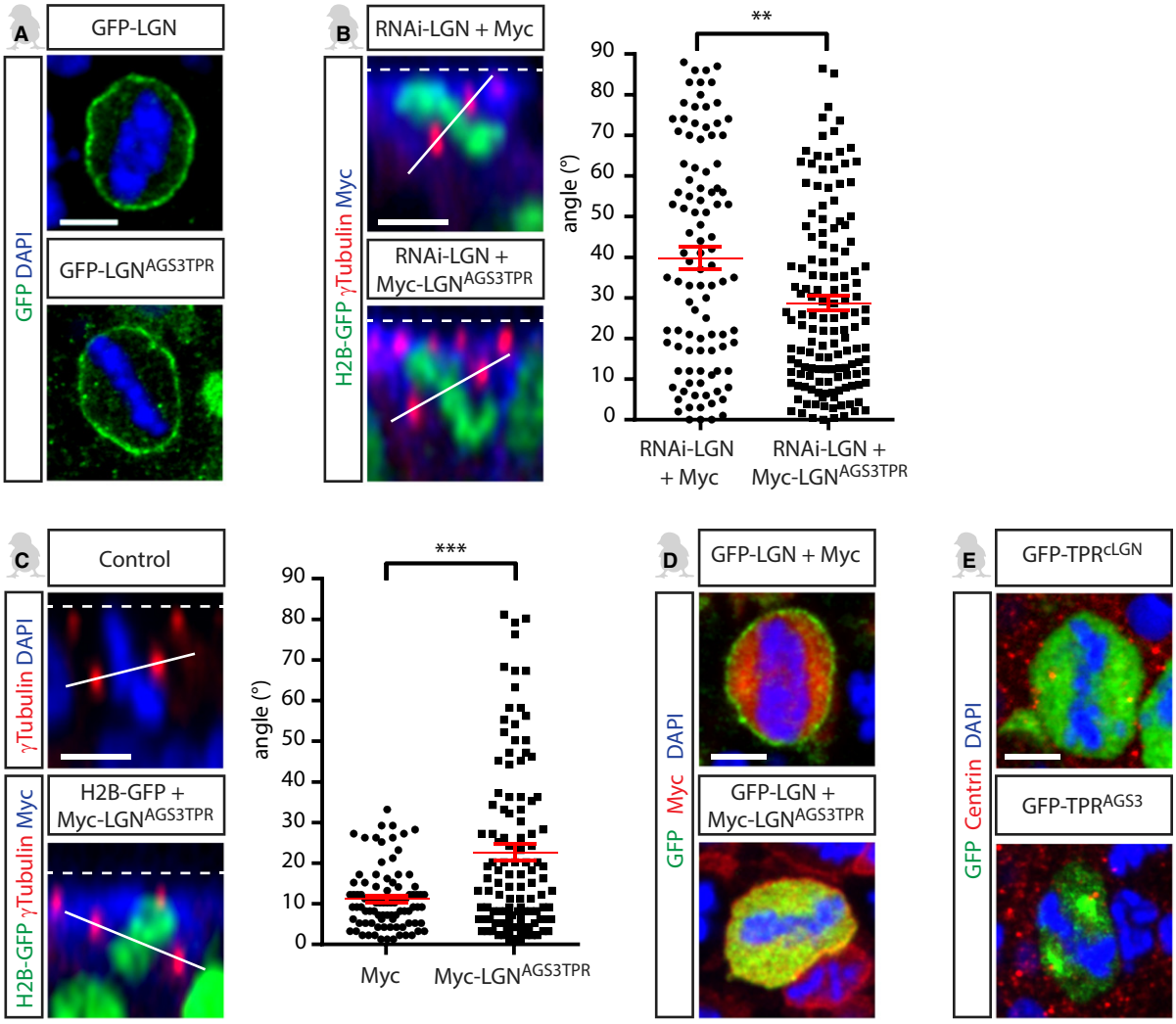


**Figure 4. TPR domains of AGS3 can partially substitute those from LGN.**

A, B LGN-TPR domain replacement by AGS3 TPR (LGN$^{AGS3TPR}$ chimera) does not affect LGN localization at the cortex (A), but the ability of this chimera to rescue LGN knockdown spindle orientation phenotype is reduced (B, quantification is provided in the right panel; mean ± SEM, $n > 100$ cells; $^{**}P < 0.01$, Mann–Whitney test) compared to wt LGN (compare with Fig 1D). Quantification for RNAi-LGN + Myc is the same as in Fig 3C as these experiments were performed on the same date.

C, D Ectopic expression of the chimera in a wt background induces spindle orientation defect (C, mean ± SEM, $n > 90$ cells; $^{***}P < 0.001$, Mann–Whitney test) and delocalizes LGN in the cytoplasm (D).

E mAGS3$^{TPR}$ is enriched at the spindle pole while cLGN$^{TPR}$ is cytoplasmic during progenitors cell division.

Data information: Scale bars: 5 μm in all panels. The dashed lines indicate the apical surface and the solid lines the mitotic spindle angle (B, C).

three functional GoLoco domains, by replacing a key arginine residue with a phenylalanine (R-F) in GoLoco 3 (LGN$^{GoLoco3m}$). Indeed, we found that this construct also had a dominant negative effect when expressed in the neuroepithelium, although weaker than Pins (Fig 5C). Conversely, we constructed a chimera composed of *Drosophila* Pins TPR and linker domains fused to mouse LGN GPR domains (dPins$^{LGN-GPR}$) and tested whether this addition of a fourth GoLoco domain in Pins would provide it with the ability to substitute for LGN. Despite its four GoLoco domains, dPins$^{LGN-GPR}$ was poorly recruited to the cortex compared to mLGN, and was completely unable to rescue the LGN loss-of-function phenotype in an RNAi background (Fig 5D).

Altogether, these data indicate that four functional GoLoco domains are necessary for LGN spindle orientation function in the vertebrate neuroepithelium. However, the inability of Pins to substitute for LGN does not only reside in its lower number of GoLoco motifs, and differences in the TPR and linker regions may also contribute to the functional differences.

A large body of work has shown that LGN and Pins both function as adaptor molecules that link force generators to the cell cortex. Their direct interaction with membrane-anchored G$\alpha_i$ subunits and NuMA/Mud is essential in this transmission chain. Previous biochemical and structural studies have shown that the two direct interactions (LGN/NuMA and LGN/G$\alpha_i$) are highly conserved

 © 2017 The Authors

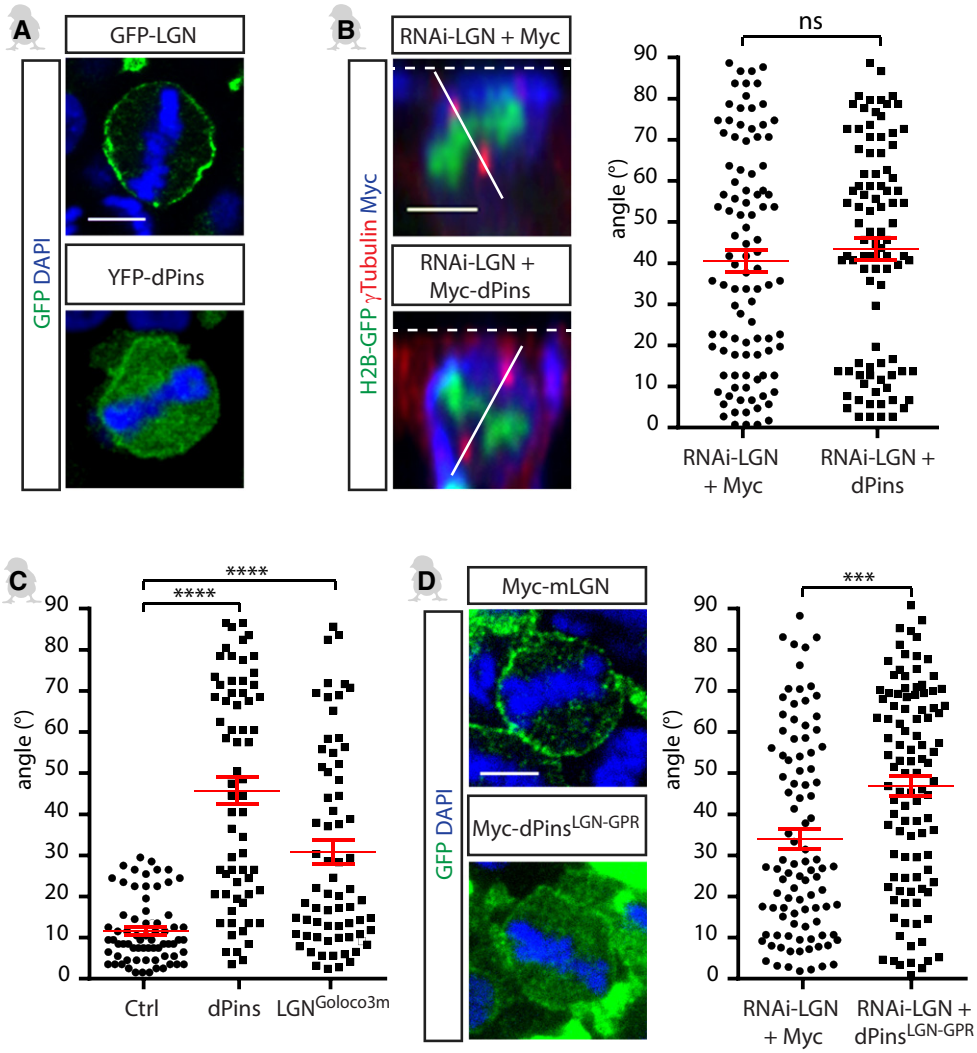


**Figure 5. *Drosophila* Pins (dPins) cannot substitute for LGN in the chick neuroepithelium.**

A, B dPins is poorly recruited at the cell cortex compared to mLGN (A) and is not able to rescue LGN loss of function during mitotic spindle orientation (B). Quantification of spindle orientations is provided in the right panel (mean ± SEM, $n > 93$ cells; ns = not significant, Mann–Whitney test). Quantification for RNAi-LGN + Myc is the same as in Fig 3C as these experiments were performed on the same date. The dashed lines indicate the apical surface and the solid lines the mitotic spindle angle.

C Quantification of mitotic spindle orientation defects after ectopic expression of dPins and $LGN^{GoLoco3\ m}$ in a wt background (mean ± SEM, $n > 95$ cells; $****P < 0.0001$, Mann–Whitney test).

D Left: Replacement of Pins GPR region (3 GoLoco) by the LGN GPR region (4 GoLoco) in the $dPins^{LGN\text{-}GPR}$ chimera does not restore cortical recruitment similar to wt LGN in chick neural progenitors. Right: $dPins^{LGN\text{-}GPR}$ is unable to rescue LGN RNAi spindle orientation phenotypes (mean ± SEM, $n > 97$ cells; $***P < 0.001$, Mann–Whitney test).

Data information: Scale bars: 5 μm in all panels.

between species, as well as between LGN and the paralogous gene AGS3 in vertebrates. Here, we have compared the ability of homologous protein modules from LGN and AGS3 to promote LGN recruitment and stability at the cell cortex. Our work reveals that these interactions must be fine-tuned to regulate force generation and spindle orientation. It also suggests that specific regulators still remain to be identified, in particular those facilitating interaction between membrane-anchored $G\alpha_i$ subunits and GoLoco motifs *in vivo*. Finally, our work illustrates that strong interactions characterized *in vitro* may not reflect the ability of endogenous proteins to interact *in vivo*, as shown by the surprising observation that GPR domains of AGS3 are not recruited to the cell cortex of dividing neuroepithelial cells at physiological levels of $G\alpha_i$ expression. Duplication of *pins* gave rise to LGN and AGS3; LGN has remained under selection pressure to maintain the canonical spindle orientation function, while AGS3 has evolved new cellular functions through a number of sequence changes. Remarkably, while those changes do not seem to affect in a major way its ability to interact *in vitro* with the two main players $G\alpha_i$ and NuMA, our analysis with chimeric constructs shows that subtle changes in distinct interaction domains

© 2017 The Authors

contribute independently to the loss of the ancestral function by AGS3.

## Materials and Methods

### Animals

Fertilized chicken eggs (JA57 strain) were obtained from EARL Morizeau and incubated at 38.5°C in a Sanyo MIR-253 incubator for appropriate durations.

Generation of the GPR-depleted AGS3 mice (AGS3ΔC) was performed as described in [8]. The targeting construct and homologous recombination strategy are described in Fig EV1. The genome after deletion of the C-terminus GPR region was confirmed by PCR and sequencing. Mouse *in utero* electroporation experiments were performed on wild-type pregnant RjOrl:SWISS females (45–50 g, Janvier LABS, Le Genest-St-Isle, France) carrying E13.5 embryos. Animals were housed under standard conditions with access to water and food *ad libitum* on a normal 12 h light/dark. Animals of both sexes were used. All animal procedures were carried out in accordance with institutional guidelines.

### Electroporation and plasmids

Electroporation in the chick neural tube was performed at embryonic day 2 (E2) as previously described [9], by applying five pulses of 50 ms at 25 V with 100 ms in between, using a square-wave electroporator (Nepa Gene, CUY21SC) and a pair of 5-mm gold-plated electrodes (BTX Genetrode model 512) separated by a 4-mm interval. For loss- and gain-of-function experiments, plasmids were used, respectively, at 2 and 1 μg/μl. For rescue experiments, 6-Myc-tagged LGN, AGS3, Pins, and chimeric expression constructs under the CAGGS promoter were added at 1 μg/μl. GFP-tagged expression constructs under the CMV promoter were used at 0.5 μg/μl.

*In utero* electroporation was performed as described previously [42]. Timed pregnant females (E13.5) were anesthetized with ketamine/xylazine and a midline laparotomy was performed, exposing uterine horns and allowing for visualizing embryos under oblique illumination; 1 μl of DNA combined with sterile Fast Green dye (1/100, Sigma) was injected with a glass capillary pipette (75–125 μm outer diameter with beveled tip) driven by an INJECT+MATIC microinjector into the lateral ventricle of each embryo. The anode of 3- or 5-mm-diameter Tweezertrodes (Sonidel Limited) was placed above the dorsal telencephalon, and four 35-V pulses of 50-ms duration were conducted across the uterine sac using a square-wave electroporator (Nepa21, Sonidel Limited). Following intrauterine surgery, the incision site was closed with sutures (4-0, Ethicon) and the mouse was allowed to recover in a clean cage. GFP-tagged expression constructs under the CMV promoter were used at 1 μg/μl, and control H2BmRFP reporter construct under the CAGGS promoter was used at 0.5 μg/μl.

Expression vectors used in this study are listed in Fig EV2.

### Immunohistochemistry

For antibody staining, chick embryos were fixed for 1 h in ice-cold 4% formaldehyde/PBS. After fixation, embryos were cut along their midline, permeabilized for 15 min in PBS/0.3% Triton X-100 (PBT 0.3%) before a 1-h blocking step in PBT 0.3%/10%FCS. Pregnant mice were euthanized 24 h after electroporation to harvest the embryonic cortex. Embryonic brains were dissected out, immersed for 2–4 h in cold 4% AntigenFix (Diapath), and rinsed in PBS. For the analysis of LGN and AGS3 subcellular localization, the neocortex on the electroporated side was dissected out and treated as whole mount. For angle measurements in the AGS3ΔC mice, whole brains were cryoprotected in 20–25% sucrose and embedded in OCT compound before cryosectioning, and treated as described in [8].

Primary antibodies used are as follows: mouse anti-Centrin (clone 20H5, Millipore #04-1624), rabbit anti-GFP (Torrey Pines Biolabs #TP401), mouse anti-γ-tubulin (clone GTU-88, Sigma #T6557), mouse anti-c-Myc (clone 9E10, Sigma #M5546), rabbit anti-c-Myc (Sigma #C3956), and rabbit anti-mouse LGN [43]. For the γ-tubulin antibody, embryos were incubated for 15-20 min in 100% acetone pre-equilibrated at −20°C, and rinsed twice in PBT 0.3% at room temperature before the blocking step. Secondary antibodies coupled to Alexa Fluor 488, Cy3, Cy5, or Alexa Fluor 647 were obtained from Jackson laboratories, and typically used at 1/500 (488 and Cy3) or 1/250 (Cy5 and 647) dilutions. DAPI (1/1,000) or Hoechst 33342 (1/1,000) was added to the secondary antibody mix. Vectashield with DAPI (Vector Laboratories) was used as a mounting medium.

### Image acquisition

Optical sections of fixed samples were obtained either on laser scanning confocal microscopes: Leica SP5 using a 40× oil immersion objective Plan Neofluar NA 1.3 and Leica LAS software, and Olympus FV1000 using a 60× water immersion objective (UPlanSApo NA 1.20), or on a spinning disk confocal microscope (Nikon Ti Eclipse inverted microscope, Yokogawa CSU-W1 confocal head, and Hamamatsu Orca Flash4LT sCMOS Camera) using a 100× oil immersion objective (APO VC, NA 1.4, Nikon). Fiji software [44] was used for image processing (Gaussian Blur) and data analysis (spindle orientation measurement, see below). When necessary, images were subjected to brightness and contrast adjustment to equilibrate channel intensities and background using Adobe Photoshop CS4 software.

### Measurement of spindle orientation in fixed samples

For chick embryos, 3D measurements of spindle orientation were obtained from the en-face mounted neuroepithelium of E3 embryos labelled with an anti-gamma-tubulin antibody to reveal spindle poles and with DAPI dye to label chromosomes, as described in [27]. Electroporated cells were identified by their expression of a Histone2B-GFP reporter protein (carried by the miRNA plasmid), also revealing the chromosomal plate of dividing cells. In addition, for rescue and dominant negative experiments, expression of Myc-tagged expression constructs was revealed by an anti-Myc antibody. En-face image stacks (0.5 μm z interval) were acquired at 40× or 100× magnification. z-views and spindle orientation quantification were done in Fiji software [44] using custom-designed macros [27]. For each experiment, mean ± SEM is provided and came from at least three embryos per condition.

 © 2017 The Authors

For mouse embryos, orientation of the mitotic spindle in anaphase was measured in cryosections from the E14.5 cortex, as described in [8].

#### Quantification of cortical signals in mitotic cells

To quantify the amount of GFP fusion proteins localized at the cell cortex of dividing chick neuroepithelial cells, we generated en-face images of cells of interest and selected the plane of the cell largest width, corresponding to the "equator". We analyzed 15 intensity profiles spanning the cell length, starting from the cell center and equally distributed along 360°. To quantify the extent of the cortical signal, we thus fitted a Gaussian profile centered on the maximum value of the profile. The fit was performed on the four adjacent pixel values around the membrane location on each profile. The integrated intensity of the fitted Gaussian was finally calculated and interpreted as the amount of protein p cortical recruitment at the membrane location on the profile. The cytoplasmic signal on a same profile was measured on $P_{cytoplasm}$ as the integrated intensity along the same line, from the cell center to the membrane location. In the end, the ratio of cortical signal over cytoplasmic signal for each of the 15 profiles was averaged to get a final relative level of protein p recruitment at the membrane in the cell of interest.

#### Protein purification and *in vitro* binding assays

Full-length human AGS3, AGS3-TPR (residues 1–341), AGS3-GoLoco (residues 340–652), human LGN-TPR (residues 1–373), and human $G\alpha_i$-ΔN (residues 26–354) were cloned into the bacterial pGEX-6PI vector (GE Healthcare), and purified by affinity on glutathione beads (GSH beads). AGS3-GoLoco and $G\alpha_i$-ΔN were cleaved from beads with PreScission protease (GE Healthcare), and further purified by anion exchange. Human His-tagged NuMA-1821–2001 was cloned into pET43 vector, and purified by nickel affinity and cation exchange.

For pull-down assays, 3 μM of GST fusion proteins was immobilized on GSH beads, and incubated for 2 h at 4°C with 10 μM of prey proteins in 10 mM Hepes pH 7.6, 0.1 M NaCl, 0.1% Triton X-100, 1 mM DTT, and 0.5 mM EDTA. After washes, proteins bound to beads were separated by SDS–PAGE and detected by Coomassie staining.

#### Statistical analysis

Statistical analyses were done using a Mann–Whitney test performed with GraphPad Prism (GraphPad software), except for chimeric GPR domains cortical intensity ratio (Fig 3G) and GFP-Dlg1 cortical intensity ratio (Fig EV3), where a one-way ANOVA test was performed. In all figures, *P*-value significances of 0.05, 0.01, 0.001, and 0.0001 are represented, respectively, by *, **, ***, and ****.

**Expanded View** for this article is available online.

### Acknowledgements
We thank Samuel Tozer and Florencia di Pietro for helpful discussions on this project. We acknowledge Benjamin Mathieu and the IBENS imaging platform for excellent assistance. Imaging equipment was acquired through the generous help of the Neuropôle de Recherche Francilien. Work in X.Morin's laboratory was supported by an INSERM Avenir Grant (R08221JS), the Fondation pour la Recherche Medicale (FRM DEQ20150331735), the Fondation ARC (ARC Livespin, SFI20111203877), the Agence Nationale pour la Recherche (ANR-12-BSV2-0014-01), Cancéropôle Ile-de-France (2013-2-INV-05), and FRC (AOE-9 2014). M. Saadaoui was the recipient of postdoctoral fellowships from INSERM (Avenir), NeRF, and ANR. This work has received support under the program "Investissements d'Avenir" launched by the French Government and implemented by the ANR, with the references: ANR-10-LABX-54 MEMO LIFE and ANR-11-IDEX-0001-02 PSL* Research University.

### Author contributions
MS and XM conceived the project. MS, RG, and XM performed experiments in chick embryos. KL performed *in utero* electroporation in mouse embryos. DK generated and analyzed AGS3ΔC mice under the supervision of FM. VJ performed the AGS3–NuMA interaction experiments under the supervision of MM. MS and XM analyzed data and wrote the manuscript.

### Conflict of interest
The authors declare that they have no conflict of interest.

## References

1. Morin X, Bellaïche Y (2011) Mitotic spindle orientation in asymmetric and symmetric cell divisions during animal development. *Dev Cell* 21: 102 – 119
2. Gillies TE, Cabernard C (2011) Cell division orientation in animals. *Curr Biol* 21: R599 – R609
3. Woodard GE, Huang NN, Cho H, Miki T, Tall GG, Kehrl JH (2010) Ric-8A and Gi{alpha} recruit LGN, NuMA, and dynein to the cell cortex to help orient the mitotic spindle. *Mol Cell Biol* 30: 3519 – 3530
4. Kotak S, Busso C, Gonczy P (2012) Cortical dynein is critical for proper spindle positioning in human cells. *J Cell Biol* 199: 97 – 110
5. Kiyomitsu T, Cheeseman IM (2012) Chromosome- and spindle-pole-derived signals generate an intrinsic code for spindle position and orientation. *Nat Cell Biol* 14: 311 – 317
6. di Pietro F, Echard A, Morin X (2016) Regulation of mitotic spindle orientation: an integrated view. *EMBO Rep* 17: 1106 – 1130
7. Mochizuki N, Cho G, Wen B, Insel PA (1996) Identification and cDNA cloning of a novel human mosaic protein, LGN, based on interaction with G alpha i2. *Gene* 181: 39 – 43
8. Konno D, Shioi G, Shitamukai A, Mori A, Kiyonari H, Miyata T, Matsuzaki F (2008) Neuroepithelial progenitors undergo LGN-dependent planar divisions to maintain self-renewability during mammalian neurogenesis. *Nat Cell Biol* 10: 93 – 101
9. Morin X, Jaouen F, Durbec P (2007) Control of planar divisions by the G-protein regulator LGN maintains progenitors in the chick neuroepithelium. *Nat Neurosci* 10: 1440 – 1448
10. Yu F, Morin X, Cai Y, Yang X, Chia W (2000) Analysis of partner of inscuteable, a novel player of *Drosophila* asymmetric divisions, reveals two distinct steps in inscuteable apical localization. *Cell* 100: 399 – 409
11. Zheng Z, Zhu H, Wan Q, Liu J, Xiao Z, Siderovski DP, Du Q (2010) LGN regulates mitotic spindle orientation during epithelial morphogenesis. *J Cell Biol* 189: 275 – 288
12. Schaefer M, Shevchenko A, Knoblich JA (2000) A protein complex containing Inscuteable and the Galpha-binding protein Pins orients asymmetric cell divisions in *Drosophila*. *Curr Biol* 10: 353 – 362

© 2017 The Authors

13. Yu F, Morin X, Kaushik R, Bahri S, Yang X, Chia W (2003) A mouse homologue of *Drosophila* pins can asymmetrically localize and substitute for pins function in *Drosophila* neuroblasts. *J Cell Sci* 116: 887 – 896
14. Wiser O, Qian X, Ehlers M, Ja WW, Roberts RW, Reuveny E, Jan YN, Jan LY (2006) Modulation of basal and receptor-induced GIRK potassium channel activity and neuronal excitability by the mammalian PINS homolog LGN. *Neuron* 50: 561 – 573
15. Sans N, Wang PY, Du Q, Petralia RS, Wang YX, Nakka S, Blumer JB, Macara IG, Wenthold RJ (2005) mPins modulates PSD-95 and SAP102 trafficking and influences NMDA receptor surface expression. *Nat Cell Biol* 7: 1179 – 1190
16. Tarchini B, Tadenev AL, Devanney N, Cayouette M (2016) A link between planar polarity and staircase-like bundle architecture in hair cells. *Development* 143: 3926 – 3932
17. Tarchini B, Jolicoeur C, Cayouette M (2013) A molecular blueprint at the apical surface establishes planar asymmetry in cochlear hair cells. *Dev Cell* 27: 88 – 102
18. Ezan J, Lasvaux L, Gezer A, Novakovic A, May-Simera H, Belotti E, Lhoumeau AC, Birnbaumer L, Beer-Hammer S, Borg JP *et al* (2013) Primary cilium migration depends on G-protein signalling control of subapical cytoskeleton. *Nat Cell Biol* 15: 1107 – 1115
19. Bhonker Y, Abu-Rayyan A, Ushakov K, Amir-Zilberstein L, Shivatzki S, Yizhar-Barnea O, Elkan-Miller T, Tayeb-Fligelman E, Kim SM, Landau M *et al* (2016) The GPSM2/LGN GoLoco motifs are essential for hearing. *Mamm Genome* 27: 29 – 46
20. Doherty D, Chudley AE, Coghlan G, Ishak GE, Innes AM, Lemire EG, Rogers RC, Mhanni AA, Phelps IG, Jones SJ *et al* (2012) GPSM2 mutations cause the brain malformations and hearing loss in Chudley-McCullough syndrome. *Am J Hum Genet* 90: 1088 – 1093
21. Walsh T, Shahin H, Elkan-Miller T, Lee MK, Thornton AM, Roeb W, Abu Rayyan A, Loulus S, Avraham KB, King MC *et al* (2010) Whole exome sequencing and homozygosity mapping identify mutation in the cell polarity protein GPSM2 as the cause of nonsyndromic hearing loss DFNB82. *Am J Hum Genet* 87: 90 – 94
22. Takesono A, Cismowski MJ, Ribas C, Bernard M, Chung P, Hazard S III, Duzic E, Lanier SM (1999) Receptor-independent activators of heterotrimeric G-protein signaling pathways. *J Biol Chem* 274: 33202 – 33205
23. Blumer JB, Oner SS, Lanier SM (2012) Group II activators of G-protein signalling and proteins containing a G-protein regulatory motif. *Acta Physiol* 204: 202 – 218
24. Kamakura S, Nomura M, Hayase J, Iwakiri Y, Nishikimi A, Takayanagi R, Fukui Y, Sumimoto H (2013) The cell polarity protein mInsc regulates neutrophil chemotaxis via a noncanonical G protein signaling pathway. *Dev Cell* 26: 292 – 302
25. De Vries L, Fischer T, Tronchere H, Brothers GM, Strockbine B, Siderovski DP, Farquhar MG (2000) Activator of G protein signaling 3 is a guanine dissociation inhibitor for Galpha i subunits. *Proc Natl Acad Sci USA* 97: 14364 – 14369
26. Kimple RJ, De Vries L, Tronchere H, Behe CI, Morris RA, Gist Farquhar M, Siderovski DP (2001) RGS12 and RGS14 GoLoco motifs are G alpha(i) interaction sites with guanine nucleotide dissociation inhibitor activity. *J Biol Chem* 276: 29275 – 29281
27. Saadaoui M, Machicoane M, di Pietro F, Etoc F, Echard A, Morin X (2014) Dlg1 controls planar spindle orientation in the neuroepithelium through direct interaction with LGN. *J Cell Biol* 206: 707 – 717
28. Bergstralh DT, Lovegrove HE, St Johnston D (2013) Discs large links spindle orientation to apical-basal polarity in *Drosophila* epithelia. *Curr Biol* 23: 1707 – 1712
29. Zhu J, Shang Y, Xia C, Wang W, Wen W, Zhang M (2011) Guanylate kinase domains of the MAGUK family scaffold proteins as specific phospho-protein-binding modules. *EMBO J* 30: 4986 – 4997
30. Sanada K, Tsai LH (2005) G protein betagamma subunits and AGS3 control spindle orientation and asymmetric cell fate of cerebral cortical progenitors. *Cell* 122: 119 – 131
31. Du Q, Macara IG (2004) Mammalian Pins is a conformational switch that links NuMA to heterotrimeric G proteins. *Cell* 119: 503 – 516
32. Peyre E, Jaouen F, Saadaoui M, Haren L, Merdes A, Durbec P, Morin X (2011) A lateral belt of cortical LGN and NuMA guides mitotic spindle movements and planar division in neuroepithelial cells. *J Cell Biol* 193: 141 – 154
33. Nipper RW, Siller KH, Smith NR, Doe CQ, Prehoda KE (2007) Galphai generates multiple Pins activation states to link cortical polarity and spindle orientation in *Drosophila* neuroblasts. *Proc Natl Acad Sci USA* 104: 14306 – 14311
34. Adhikari A, Sprang SR (2003) Thermodynamic characterization of the binding of activator of G protein signaling 3 (AGS3) and peptides derived from AGS3 with G alpha i1. *J Biol Chem* 278: 51825 – 51832
35. Jia M, Li J, Zhu J, Wen W, Zhang M, Wang W (2012) Crystal structures of the scaffolding protein LGN reveal the general mechanism by which GoLoco binding motifs inhibit the release of GDP from Galphai. *J Biol Chem* 287: 36766 – 36776
36. Willard FS, Zheng Z, Guo J, Digby GJ, Kimple AJ, Conley JM, Johnston CA, Bosch D, Willard MD, Watts VJ *et al* (2008) A point mutation to Galphai selectively blocks GoLoco motif binding: direct evidence for Galpha.GoLoco complexes in mitotic spindle dynamics. *J Biol Chem* 283: 36698 – 36710
37. Culurgioni S, Alfieri A, Pendolino V, Laddomada F, Mapelli M (2011) Inscuteable and NuMA proteins bind competitively to Leu-Gly-Asn repeat-enriched protein (LGN) during asymmetric cell divisions. *Proc Natl Acad Sci USA* 108: 20998 – 21003
38. Yuzawa S, Kamakura S, Iwakiri Y, Hayase J, Sumimoto H (2011) Structural basis for interaction between the conserved cell polarity proteins Inscuteable and Leu-Gly-Asn repeat-enriched protein (LGN). *Proc Natl Acad Sci USA* 108: 19210 – 19215
39. Zhu J, Wen W, Zheng Z, Shang Y, Wei Z, Xiao Z, Pan Z, Du Q, Wang W, Zhang M (2011) LGN/mInsc and LGN/NuMA complex structures suggest distinct functions in asymmetric cell division for the Par3/mInsc/LGN and Galphai/LGN/NuMA pathways. *Mol Cell* 43: 418 – 431
40. Pan Z, Shang Y, Jia M, Zhang L, Xia C, Zhang M, Wang W, Wen W (2013) Structural and biochemical characterization of the interaction between LGN and Frmpd1. *J Mol Biol* 425: 1039 – 1049
41. Carminati M, Gallini S, Pirovano L, Alfieri A, Bisi S, Mapelli M (2016) Concomitant binding of Afadin to LGN and F-actin directs planar spindle orientation. *Nat Struct Mol Biol* 23: 155 – 163
42. Loulier K, Lathia JD, Marthiens V, Relucio J, Mughal MR, Tang SC, Coksaygan T, Hall PE, Chigurupati S, Patton B *et al* (2009) beta1 integrin maintains integrity of the embryonic neocortical stem cell niche. *PLoS Biol* 7: e1000176
43. Kaushik R, Yu F, Chia W, Yang X, Bahri S (2003) Subcellular localization of LGN during mitosis: evidence for its cortical localization in mitotic cell culture systems and its requirement for normal cell cycle progression. *Mol Biol Cell* 14: 3144 – 3155
44. Schindelin J, Arganda-Carreras I, Frise E, Kaynig V, Longair M, Pietzsch T, Preibisch S, Rueden C, Saalfeld S, Schmid B *et al* (2012) Fiji: an open-source platform for biological-image analysis. *Nat Methods* 9: 676 – 682


 © 2017 The Authors